

# In Situ Measurement of Fatigue Crack Growth Rates in a Silicon Carbide Ceramic at Elevated Temperatures Using a DC Potential System

Authorized Reprint from Journal of Testing and Evaluation, July 2000 ©Copyright 2000  
American Society for Testing and Materials, 100 Barr Harbor Drive, West Conshohocken, PA 19428-2959

**REFERENCE:** Chen, D., Gilbert, C. J., and Ritchie, R. O., "In Situ Measurement of Fatigue Crack Growth Rates in a Silicon Carbide Ceramic at Elevated Temperatures Using a DC Potential System," *Journal of Testing and Evaluation*, JTEVA, Vol. 28, No. 4, July 2000, pp. 236–241.

**ABSTRACT:** The understanding of the mechanisms of fatigue-crack propagation in advanced ceramics at elevated temperatures (>800°C) has in part been hampered by the experimental difficulty in directly measuring crack lengths, and hence crack growth rates, at such high temperatures. In this study, we show how the direct-current (DC) electrical-potential technique, which has been used for such measurements in metallic materials for over 30 years, can be successfully utilized to monitor fatigue crack growth rates in situ in a silicon carbide ceramic at temperatures between 850 to 1300°C, because of the electrical conductivity in SiC at these temperatures. In addition to providing a highly efficient means of collecting such data, this approach offers several significant advantages over the techniques that have been used to date for advanced ceramics, particularly in avoiding artifacts due to thermal fatigue and oxidation from repeated exposure to air and/or lower temperatures while making measurements. Effects of parameters such as load ratio and loading frequency are examined, both on crack growth behavior and the accuracy of measurement. With appropriate considerations, electrical-potential calibrations determined at ambient temperatures in metallic materials can be readily applied to elevated temperature measurements in silicon carbide.

**KEYWORDS:** crack monitoring, electrical-potential method, ceramics, fatigue crack propagation, elevated temperatures

Accurate and continuous measurements of crack lengths and, hence crack growth rates are critical for experimental studies on subcritical crack growth by fatigue, creep or environmentally assisted cracking. Although a number of successful techniques have been developed for the in situ monitoring of crack extension at ambient temperatures [1–4], few are successful at elevated temperatures [5]. One notable success is the direct-current (DC) electrical-potential technique, which has been used for metallic materials for over 30 years [6–8] and as such has been adopted for high-temperature crack initiation and propagation studies typically at temperatures less than 650°C [9–11], primarily because of its simplicity, applicability and relatively low cost.

Corresponding measurements of subcritical crack growth studies in nonconducting materials, such as ceramics, however, have

been confined to visual and elastic compliance methods or techniques involving conducting metallic foils affixed or evaporated on the test specimen surface [e.g., 12–14]. Because most of these techniques are largely ineffective at the elevated temperatures pertinent to ceramics, i.e., from 850 to 1300°C and greater, the characterization of subcritical crack growth behavior in ceramics at these industrially relevant temperatures has been quite limited. Although laser interferometric [15] and high-temperature [16] displacement gages have been developed, currently the vast majority of cyclic fatigue crack extension measurements in ceramics at elevated temperatures greater than 800°C have involved optical (visual) measurements, invariably achieved following periodic cooling of the specimens. Since this can lead to extraneous effects from thermal fatigue and oxidation from repeated exposure to air, there is a clear need for a direct in situ measurement technique, which provides greater efficiency in collecting data.

Because most advanced ceramics are, in general, electrically non conductive, the electrical-potential method has not to date been considered as a serious crack-monitoring technique. However, in the current work, we show that whereas this is the case for ambient temperature behavior, at elevated temperatures some advanced ceramics such as silicon carbide display sufficient electrical conductivity so that the electrical-potential technique can be utilized as a highly efficient method for the continuous, in situ monitoring of crack-growth rates at temperatures between ~800 and 1300°C.

## Experimental Procedures

### *Material and Test Specimens*

The material under investigation was an in situ toughened, monolithic silicon carbide, hot-pressed at 1900°C for 1 h at 50 MPa pressure with additions (in wt%) of 3Al-0.6B-2C (termed ABC-SiC). The resulting microstructure consisted of a three-dimensional interlocking network of elongated plate-like grains. Details of material processing and microstructural characterization have been presented elsewhere [17]. Cyclic fatigue-crack growth tests were performed using 3-mm-thick disk-shaped compact-tension DC(T) specimens with a width of ~28 mm, a geometry that conforms to the ASTM Standard Test Method for Measurement of Fatigue Crack Growth Rate (E 647-95a).

### *Elevated-Temperature Cyclic Fatigue Testing*

To evaluate the crack-monitoring technique, specimens were cycled at 850, 1200 and 1300°C, at a range of load ratios (load ratio =  $R = P_{\min}/P_{\max}$ , where  $P_{\min}$  and  $P_{\max}$  are the minimum and max-

Manuscript received: 10/12/99; manuscript accepted 03/15/00.

<sup>1</sup> Materials Sciences Division, Lawrence Berkeley National Laboratory and Department of Materials Science and Mineral Engineering, University of California, Berkeley, CA 94720

imum applied loads, respectively, during a loading cycle) from  $R \sim 0.1$  to  $0.5$  and loading frequencies (sinusoidal waveform) from  $\nu \sim 3$  to  $25$  Hz, in general accordance with E 647. Specifically, tests were conducted under automated stress intensity,  $K$ , control at a constant load ratio, with growth rates monitored under decreasing stress intensity range  $\Delta K$  ( $\Delta K = K_{\max} - K_{\min}$ , where  $K_{\max}$  and  $K_{\min}$  are the maximum and minimum stress intensity factors, respectively, during a loading cycle) conditions with a normalized  $K$ -gradient<sup>2</sup> set to  $-0.08 \text{ mm}^{-1}$ . Prior to testing, the DC(T) test specimens were fatigue precracked at room temperature for several millimeters beyond the half-chevron-shaped starter notch; this notch geometry was used to facilitate crack initiation.

All tests were performed on a computer-controlled commercial servo-hydraulic mechanical testing system in an environmental chamber/furnace, heated by graphite elements that maintain temperature to within  $\pm 1^\circ\text{C}$ , with an environment of flowing gaseous argon at atmospheric pressure. Heating and cooling rates were kept at  $10^\circ\text{C}/\text{min}$  to minimize any thermal shock effects. After reaching the desired temperature and prior to commencing the test, the furnace temperature was kept constant for 1 to 3 h to permit the thermal equilibrium of the system.

Crack lengths at elevated temperatures were monitored in situ using the electrical-potential method, as described in the following section. To verify such measurements, readings were checked using an optical microscope. For comparison, room-temperature cyclic fatigue-crack growth rates were also measured using the back-face strain elastic-unloading compliance method [18,19], using a  $350 \Omega$  strain gage affixed to the back surface of the specimen.

#### Crack Length Measurements using Electrical-Potential Methods

**Principle of the electrical-potential technique**—The electrical-potential technique is based on the phenomenon that the presence of a crack in an electrical field can introduce a disturbance that can be interpreted in terms of crack size and shape of specimen. When applied to the crack-growth monitoring, the method entails passing a constant direct- or alternating-current through a cracked test specimen, and measuring the change in electrical potential across the crack as it propagates (Fig. 1). With increasing crack length, the uncracked cross-sectional area of the test piece decreases, its electrical resistance increases, and thus the potential difference between two points spanning the crack rises. By monitoring this increasing potential,  $V$ , and comparing it with the reference potential,  $V_0$ , the ratio of crack length to width,  $a/W$ , can be determined through the use of the relevant calibration curve for the particular test-specimen geometry concerned. In practice, the crack length is expressed as a function of the normalized potential ( $V/V_0$ ) and the initial crack length ( $a_0$ ). Through the use of such nondimensional ratio, calibration curves become independent of material properties, specimen thickness, and magnitude of input current. Hence, the same calibration equation can, in principle, be used for different materials, provided the same specimen geometry and current input/potential measurement probe locations are maintained.

**Unique Feature of Electrical Resistivity in SiC**—As noted above, electrical-potential methods have not been utilized for ceramics as they are invariably non-conducting, although at lower

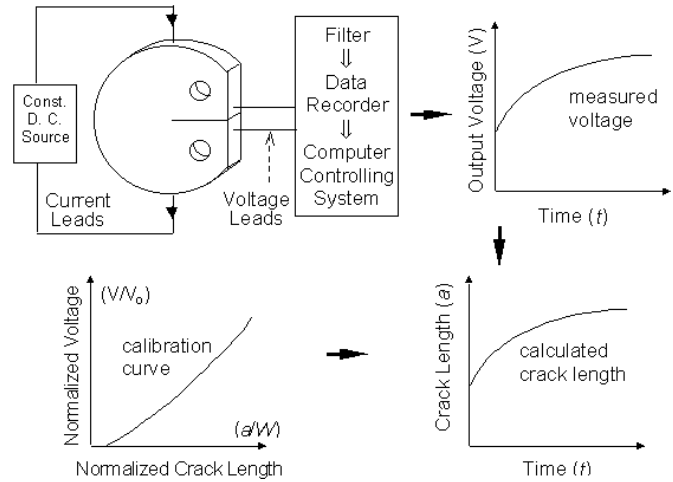


FIG. 1—Schematic illustration showing the principle and experimental setup for the electrical-potential method for in situ monitoring of crack extension.

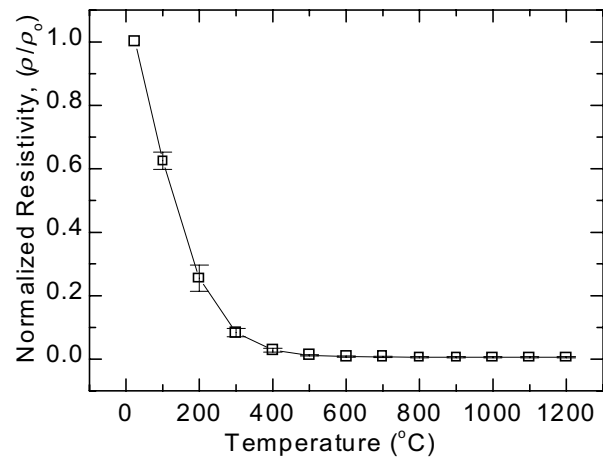


FIG. 2—Relationship between electrical resistivity,  $\rho$ , and temperature in the SiC, where  $\rho_0$  is the resistivity at room temperature. Note that the electrical resistance drops dramatically with increasing temperature and then stays almost constant at temperatures greater  $\sim 600^\circ\text{C}$ .

temperatures conducting metal foils can be affixed to specimen surfaces to monitor crack advance [12,13]. Silicon carbide, however, does display some degree of electrical conductivity. At room temperature, its electrical resistivity ( $\rho \sim 10^4 \Omega\cdot\text{cm}$ ) is too high to use the method effectively. At elevated temperatures, on the other hand, there are roughly three-orders-of-magnitude decrease in the resistivity, i.e.,  $\rho \sim 10^1 \Omega\cdot\text{cm}$  at temperatures greater than  $600^\circ\text{C}$  (Fig. 2), such that the technique can be usefully applied.

**Experiment Setup and Measurement Procedures**—Using the experiment setup shown in Fig. 1, a constant direct current of  $\sim 400$  to  $800$  mA generated by a stabilized DC voltage supply was passed through the DC(T) sample. With an electrical resistance between the potential leads of  $20$  to  $50 \Omega$  ( $\rho \sim 10 \Omega\cdot\text{cm}$ ) at temperatures greater than  $600^\circ\text{C}$ , a corresponding initial output potential of  $0.4$  to  $1.0$  V was developed across the notch mouth. Subsequent changes in this potential were then measured continuously to per-

<sup>2</sup> The  $K$ -gradient is a factor that defines the rate at which the stress intensity  $K$  will increase or decrease with crack extension during a fatigue test. The applied stress intensity range is governed by the equation,  $\Delta K_c = \Delta K_i \exp[K\text{-gradient}(a_c - a_i)]$ , where the subscripts "c" and "i" indicate the current and initial values of the associated variable, and  $a$  is the crack length.

mit in situ monitoring of crack length. Electrical-potential calibrations for this specimen geometry, given in Ref. 19, were used to compute crack lengths.

To reduce background electrical noise, the output voltage was first passed through a filter with low-pass cutoff frequency of 1 to 10 Hz. The voltage signal was monitored using a digital nanovoltmeter (resolution  $\sim 0.1 \mu\text{V}$ ), displayed on a strip chart plotter, and fed into a computerized fatigue test controlling system which instantaneously calculated the crack length according to the measured output potential and the calibration curve. The no-current voltage was measured periodically to determine the thermal voltage such that the output voltage could be compensated. Care was taken to maintain a single ground in the electrical measurement set up to further minimize noise levels.

**Measurement Accuracy**—Measurement accuracy may be affected by a number of factors, including the electrical stability and resolution of the potential measurement system, joining between the test specimen and the current input potential measurement leads, electrical insulation of the specimen from the loading device, electrical contact between crack surfaces due to crack closure and/or bridging of uncracked segments, changes of electrical resistivity with microstructural evolution, temperature variations, or both. The influence of these factors is described as follows.

**Connection Between Specimen and Current and Potential Leads**—One of the key points for making successful electrical-potential measurements at elevated temperatures is the reliable connection between the ceramic specimen and metallic current input and potential measurement leads. To reduce errors from variations in the contact resistance, the leads must be firmly attached to the specimen and maintain a good electrical contact at elevated temperatures under prolonged cyclic loading. In the present study, a two-layer joining method using ultrahigh-temperature adhesives was adopted, as illustrated schematically in Fig. 3. First, a graphite adhesive layer connecting the 100- $\mu\text{m}$ -diameter-high purity molybdenum leads to the test specimen was made to ensure a good electrical contact. After thermal curing at 200°C for 2 h, the graphite layer was then covered by a thin layer of alumina adhesive to provide oxidation protection for the graphite layer. Furthermore, in order to strengthen the joint, small notches of  $\sim 0.5$  mm in depth and  $\sim 0.12$  mm in width were cut on the edges of

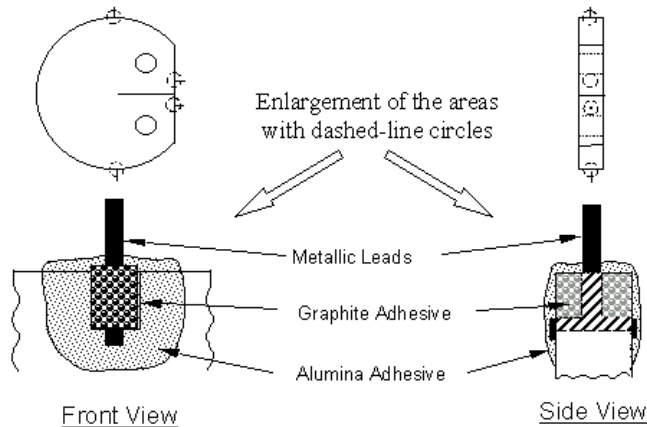


FIG. 3—Schematic illustration showing the connection between the SiC sample and the metallic current input and potential measurement leads using high-temperature graphite and alumina adhesives.

specimens where the ends of metallic leads were embedded before coatings with adhesive.

To optimize sensitivity (the ability to discriminate between small differences in crack length), reproducibility (inaccuracies produced by small errors in positioning the potential leads) and measurability (the signal-to-noise ratios which largely depends on the magnitude of output voltage signal), as described in Ref. 20, the potential leads were placed on the notched side of DC(T) specimen,  $\sim 1$  mm away from the central line, as recommended by E 647; the current input leads were placed on the top and bottom sides in order to securely anchor their connections, as illustrated in Fig. 1.

**Insulation of Specimen from the Loading Device**—To ensure accurate potential readings, it is generally necessary that the specimen constitutes the only conducting path for the DC current; i.e., the specimen is electrically insulated from the testing machine or any other component to which it is attached. In the present experiments, as the high-temperature loading rods were made of graphite, which is conducting, the specimen was electrically isolated using nonconducting, high-purity alumina loading pins; this ensured that the electrical resistance of the loading device was a factor of approximately  $10^4$  times larger than that of the specimen. Note that for operation at high temperatures it is critically important to use high-purity materials for the various loading, insulator and measurement components as lower-purity materials can be prone to erratic changes in conductivity at these temperatures.

**Effect of Thermal EMFs**—One of the prime difficulties with DC electrical-potential techniques is the junction potentials created at points of current and potential lead attachment. To avoid such thermal electromotive forces (EMFs), potential leads are ideally made from the same material as the specimen. With advanced ceramics, this is clearly not feasible. In this study, where high-purity molybdenum wires (insulated by ceramic sleeves) were used, it was necessary to measure and correct for the thermal EMFs by taking a potential reading at zero current; this voltage was then offset using a signal conditioner which also served as a filter to reduce noise.

**Crack Closure and Grain Bridging Effects**—A characteristic of many monolithic ceramics, such as  $\text{Al}_2\text{O}_3$ ,  $\text{Si}_3\text{N}_4$  and SiC, is that they can develop a zone of interlocking grain bridges behind the crack tip; indeed, such bridging constitutes their primary (extrinsic) toughening mechanism, which then degrades under cyclic loading [e.g., 14]. Such bridging results in crack surface contact close to the crack tip, akin to crack closure behavior in metals [21], and is particularly prevalent in the ABC-SiC evaluated in this study [22]. This phenomenon results in an electrically conducting path behind the crack front, leading to underestimates of the actual crack length. Moreover, depending upon the loading frequency and the response of the measurement device, such bridging can also cause significant changes in the electrical potential during the loading cycle. Indeed, in the present study, variations in the potential during the cycle led to variations in measured crack lengths of typically 0.05 mm or more.

To minimize these effects, (1) potential readings were taken at the peak load during the loading cycle, and (2) a linear correction for such electrical shorting and other sources of error was made through comparison to the actual final crack length, measured optically at the completion of the test, as described below.

**Precision and Stability of Measurements**—Because of their low resistivity,  $\sim 10^{-11} \Omega\text{-cm}$ , typical output voltages in metallic materials are in the microvolt range, even with applied currents as large as  $\sim 50 \text{ A}$ . This necessitates the use of an amplifier, with the gain of  $10^3$  to  $10^4$ , to enhance output voltages prior to measurement. However, with SiC ceramics at temperatures greater than  $600^\circ\text{C}$ , the resistivity is  $\sim 10 \Omega\text{-cm}$ , such that a relatively small current ( $< 1 \text{ A}$ ) produces an output voltage across the notch of  $\geq 1 \text{ V}$ . Such a larger output voltage in SiC obviates the use of signal amplifiers, with the usual problems of long-term “drift”. In addition the signal-to-noise ratio is markedly improved, thereby making measurements more reliable.

Another consideration for testing at elevated temperatures is to ensure that the temperature of the test specimen is constant and uniform, especially between the potential measurement leads, as this can result in false indications of crack length changes. This effect is minimal with SiC, however, as the resistivity is essentially independent of temperature at greater than  $600^\circ\text{C}$  (Fig. 2).

**Validation of the Calibration to Elevated Temperatures**—Finally, there is the issue of calibration and the applicability of experimental room-temperature calibrations [e.g., 6,7,19,20] for elevated temperature use. In principle, electrical-potential calibrations are independent of temperature, provided it is constant. At elevated temperatures, however, time-dependent creep deformation, microstructural changes, and the buildup or breakdown of corrosion products inside the growing crack can all affect the electrical resistivity. However, the oxidation resistance of SiC at 1200 to  $1300^\circ\text{C}$  is high and the steady-state creep rates,  $\dot{\epsilon}$ , are relatively low, i.e.,  $\dot{\epsilon} < 6 \times 10^{-10} \text{ s}^{-1}$  at an applied stress of  $100 \text{ MPa}$  [23], such that problems from these effects are minimized.

## Results and Discussion

Using the electrical-potential method to monitor crack lengths, cyclic fatigue-crack growth rates in ABC-SiC at 850, 1200 and  $1300^\circ\text{C}$  are shown in Fig. 4 as a function of the applied stress intensity range,  $\Delta K$ , for loading frequencies of 3 and 25 Hz, and load ratios of 0.1 and 0.5. Corresponding results at  $25^\circ\text{C}$ , where crack lengths were measured using back-face strain compliance, are shown for comparison. A detailed mechanistic description of cyclic fatigue-crack growth behavior in ABC-SiC is presented elsewhere [24].

To examine the accuracy of such measurements, crack lengths determined from the electrical-potential method were compared with those measured using an optical microscope at the completion of the test. Generally, it was found that lengths determined using the electrical-potential method were less than the optically measured values due to the various sources of error sources described above. Assuming the optically measured crack lengths were the actual crack lengths, a linear correction factor was used to quantify this underestimate and to “correct” the raw data

$$\Delta a = \Delta a_p (1 + \delta_a / \Delta a_{pf}) \quad (1)$$

where  $\Delta a$  is the crack extension at any instant;  $\Delta a_p$  is the crack extension determined from the electrical potential output,  $\delta_a$  is the discrepancy in the optically measured and electrical-potential determined final crack extension, and  $\Delta a_{pf}$  is the final crack extension determined from the electrical-potential method. The value of the correction factor increases linearly (the choice of the linear function is arbitrary) between zero at the initial crack length to a maximum at the final crack length.

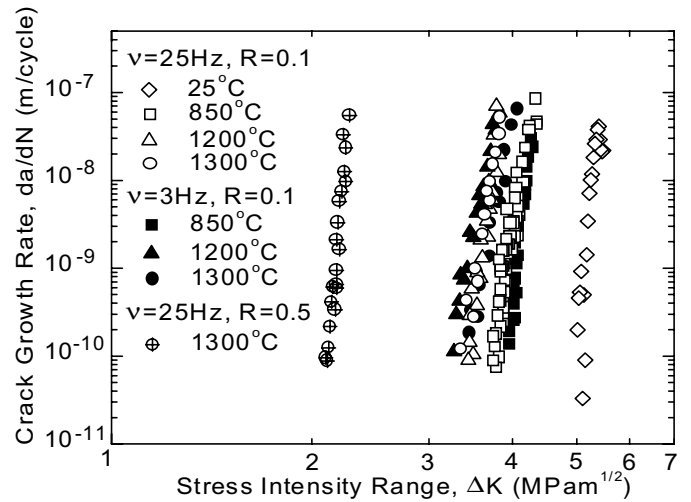


FIG. 4—Cyclic fatigue-crack growth rates,  $da/dN$ , in ABC-SiC as a function of the applied stress-intensity range  $\Delta K$ , at temperatures between 25 and  $1300^\circ\text{C}$  at frequencies of 3 and 25 Hz and load ratios of 0.1 and 0.5. Results at 850 to  $1300^\circ\text{C}$  were derived from electrical-potential measurements; corresponding results at  $25^\circ\text{C}$  involved crack length monitoring using back-face strain compliance.

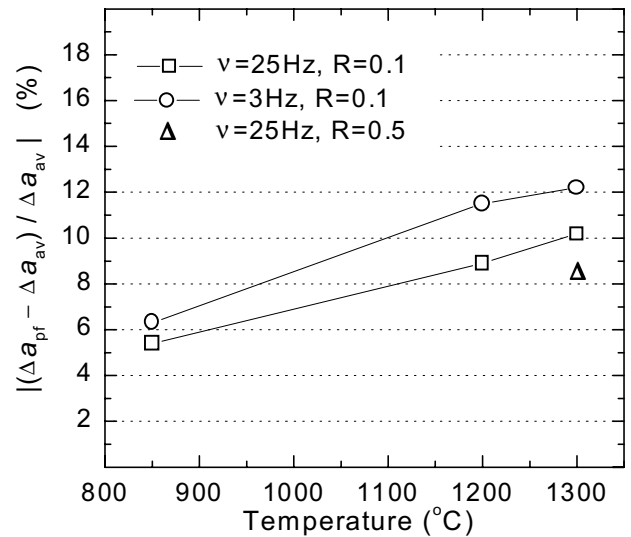


FIG. 5—Absolute value of the percent discrepancy,  $|(\Delta a_{pf} - \Delta a_{av}) / \Delta a_{av}|$ , between values of final crack extension determined from electrical-potential measurements,  $\Delta a_{pf}$ , and the mean crack extension value measured optically on the specimens after testing,  $\Delta a_{av}$ .

Figure 5 shows the absolute discrepancy, defined as  $|(\Delta a_{pf} - \Delta a_{av}) / \Delta a_{av}|$ , between values of the final crack extension determined from electrical-potential measurements,  $\Delta a_{pf}$ , and the average values measured on the test specimens after testing using an optical microscope,  $\Delta a_{av}$ . The total crack extension for each test was 2 to 3 mm. It is apparent that the error increases with increasing temperature and decreasing load ratio and is somewhat greater at 3 Hz compared to 25 Hz. Quantitatively, the discrepancy between optically measured and crack extensions determined from the electrical potential method range from 5 to 6% at  $850^\circ\text{C}$  to 9 to 12% at 1200 to  $1300^\circ\text{C}$ . Such a magnitude of error, 5 to 12%, refers to the crack extension. The corresponding error in terms of the total crack length is much smaller, being 1 to 3% in terms of the size of spec-

imens used in this study. In practice, before the crack started to grow, i.e., below the fatigue crack-growth threshold  $\Delta K_{th}$ , the input reference potential was adjusted to make the output calculated crack length equal to the actual initial crack length  $a_0$ . In this study, roughly twenty measurements were conducted in ABC-SiC, and the measurement errors in crack length in all experiments were within the range stated above.

Noted that the effect of such measurement errors in crack length on the subsequent calculation of stress intensity range  $\Delta K$  and crack growth rate  $da/dN$  are small. By using an average crack length of  $\sim 13$  mm and total crack extension of  $\sim 2.5$  mm during fatigue for the size of DC(T) specimens used in this study, a 5 to 12% measurement error in the crack extension (or 1 to 3% error in the total crack length) translated to a change in the value of corresponding stress intensity range  $\Delta K$  of only 0.05 to 0.15 MPa $\sqrt{m}$ . Such a magnitude of error in  $\Delta K$  will not essentially affect the characterization of the cyclic fatigue-crack growth behavior. Furthermore, after the raw data of crack length were "corrected" using Eq 1, the error of calculated  $\Delta K$  was negligible. Since the relative influence of such crack length measurement errors on the calculated crack growth rate is even smaller, we conclude that the magnitude of error in the crack length using this technique does not compromise the generation of accurate crack growth rate versus  $\Delta K$  data.

As discussed in previous section, several phenomena that occurred at elevated temperatures may account for such variations in measurement accuracy. First, at temperatures greater than  $\sim 1100^\circ\text{C}$ , there can be a marked decrease in the resistivity of the loading pins and/or wire insulators, which lowers relative resistance of the specimen compared to the loading path by two orders of magnitude. Second, the magnitude of thermal EMFs from dissimilar material junctions increases. Third, greater measurement errors at 3 Hz, compared to 25 Hz, frequencies probably resulted from the extended testing time at the lesser frequency, i.e., typically a 3 Hz test may last  $\sim 10$  days compared to  $\sim 2$  days at 25 Hz. Longer duration at elevated temperatures, especially at  $1200^\circ\text{C}$  and above, can cause greater thermal EMFs drift, and in general make it more difficult to maintain the electrical stability of the potential measurement system. For example, although the graphite layer used to bond the metallic wires to the test specimen has an alumina coating, oxidation can occur leading to changes in the contact resistance and hence the reference voltage,  $V_0$ . Lastly, the lower accuracy at  $R = 0.1$ , compared to  $R = 0.5$ , can be attributed to reduced crack surface contact, and hence less electrical shorting, at the greater load ratio.

Note finally that although in principle there is no upper temperature limit for the use of the electrical-potential crack-monitoring technique, in practice we have found that to successfully minimize the many sources of error described above for conducting ceramics, it is difficult to operate at temperatures much greater than  $1300^\circ\text{C}$  without severely compromising the claimed accuracy of 5 to 12% on crack extension measurements.

## Conclusions

In the present work, the DC electrical-potential crack-monitoring method was utilized to continuously monitor cyclic fatigue crack growth rates in situ at elevated temperatures,  $850$  to  $1300^\circ\text{C}$ , in an advanced SiC ceramic that displays some degree of electrical conductivity (indeed this method is also being used currently for other brittle materials, including  $\text{Ti}_3\text{SiC}_2$  and Mo-12Si-8.5B). In addition to the usual requirements of a stable system for measuring electrical potential and a constant current supply, the technique was

shown to provide reasonable accurate results if (1) contact resistances (where the current leads attach to the specimen) were minimized through the use of coated high-temperature adhesives; (2) thermal EMFs were minimized and accounted for by periodic measurement; (3) the specimen was electrically insulated from the test machine; and (4) allowance was made for electrical shorting between mating crack surfaces due to crack bridging and crack closure phenomena. Using these precautions and a room-temperature experimental calibration, an accuracy on absolute crack extension measurement of 5 to 12% (1 to 3% error in the total crack length in terms of the specimens used in this study) was attained for operations up to a practical upper limit in temperature of  $\sim 1300^\circ\text{C}$ .

## Acknowledgments

This work was supported by the Director, Office of Science, Office of Basic Energy Sciences, Materials Sciences Division of the U.S. Department of Energy under Contract No. DE-AC03-76SF00098. The first author would additionally like to acknowledge the support of Berkeley Scholars Program. Thanks are due to Dr. J. M. McNaney for his help with experimentation.

## References

- [1] *The Measurement of Crack Length and Shape during Fracture and Fatigue*, C. J. Beevers, Ed., EMAS Ltd., Warley, UK, 1980.
- [2] *Fatigue Crack Measurement: Techniques and Applications*, K. J. Marsh, R. A. Smith, R. O. Ritchie, Eds., EMAS Ltd., Warley, U.K., 1991.
- [3] Saxena, A. and Muhlstein, C. L., "Fatigue Crack Growth Testing," in *ASM Handbook, Volume 19, Fatigue and Fracture*, S. R. Lampman, Ed., The Materials Information Society, 1996, pp. 168-184.
- [4] Wei, R. P. and Brazill, R. L., "An A.C. Potential System for Crack Length Measurement" in *The Measurement of Crack Length and Shape During Fracture and Fatigue [Proc. Conf]*, Birmingham, England, May 1997, 1980, pp. 190-201.
- [5] Saxena, A., "Electrical Potential Technique for Monitoring Subcritical Crack Growth at Elevated Temperature," *Eng. Fract. Mech.*, Vol. 13, No. 4-D, 1980, pp. 741-750.
- [6] Johnson, H. H., "Calibrating the Electrical Potential Method for Studying Slow Crack Growth," *ASTM Mater. Res. Stand.*, Vol. 5, No. 9, 1965, pp. 442-445.
- [7] Li, Che-Yu and Wei, R. P., "Calibrating the Electrical Potential Method for Studying Slow Crack Growth," *ASTM Mater. Res. Stand.*, Vol. 6, No. 8, 1966, p. 392.
- [8] Ritchie, R. O., Garrett, G. G. and Knott, J. F., "Crack Growth Monitoring: Optimization of the Electrical Potential Technique Using an Analogue Method," *Int. J. Fract. Mech.*, Vol. 7, No. 4, 1971, pp. 462-467.
- [9] Liaw, P. K., Saxena, A. and Schaefer, J., "Estimating Remaining Life of Elevated-Temperature Steam Pipes - Part I. Materials Properties," *Eng. Fract. Mech.*, Vol. 32, No. 5, 1989, pp. 675-708.
- [10] Freeman, B. L. and Neate, G. J., "The Measurement of Crack Length during Fracture at Elevated Temperatures using the d.c. Potential Drop Technique," in: *The Measurement of Crack Length and Shape during Fracture and Fatigue*, C. J. Beevers, Ed., EMAS, Engineering Materials Advisory Service Ltd., 1980, pp. 435-459.
- [11] Liaw, P. K., Rao, G. V. and Burke, M. G., "Creep Fracture Behavior of 2.25Cr-1Mo Welds from a 31-year-old Fossil

- Power Plant," *Mater. Sci. Eng.*, Vol. A131, 1991, pp. 187-201.
- [12] Dauskardt, R. H. and Ritchie, R. O., "Cyclic Fatigue Crack Growth Behavior in Ceramics," *Closed Loop*, Vol. 17, 1989, pp. 7-17.
- [13] Dauskardt, R. H., Marshall, D. B. and Ritchie, R. O., "Cyclic Fatigue-Crack Propagation in Magnesia-Partially-Stabilized Zirconia Ceramics," *Journal Am. Ceram. Soc.*, Vol. 73, No. 4, 1990, pp. 893-903.
- [14] Gilbert, C. J., Dauskardt, R. H. and Ritchie, R. O., "Behavior of Cyclic Fatigue Cracks in Monolithic Silicon Nitride," *Journal Am. Ceram. Soc.*, Vol. 78, No. 9, 1995, pp. 2291-2300.
- [15] Jenkins, M. G., Kobayashi, A. S. and Bradt, R. C., "Crack Length Measurements of Ceramics at Elevated Temperatures using the Laser Interferometric Displacement Gauge," *Fatigue Crack Measurement: Techniques and Applications*, K. J. Marsh, R. A. Smith, and R. O. Ritchie, Eds., EMAS Ltd., Warley, U.K., 1991, pp. 335-373.
- [16] Haubensak, F. G., Bhatnagar, A. and Dauskardt, R.H., "Subcritical Growth of Microstructurally Small Cracks in Silicon Nitride Ceramics," *Small Fatigue Cracks: Mechanics, Mechanisms and Applications*, K.S. Ravichandran, R.O. Ritchie, and Y. Murakami, Eds., Elsevier, Oxford, UK, 1999, pp. 271-282.
- [17] Cao, J. J., MoberlyChan, W. J., De Jonghe, L. C., Gilbert, C. J. and Ritchie, R. O., "In Situ Toughened Silicon Carbide with Al-B-C Additions," *Journal Am. Ceram. Soc.*, Vol. 79, No. 2, 1996, pp. 461-469.
- [18] Maxwell, D. C., "Strain Based Compliance Method for Determining Crack Length for a C(T) Specimen," Technical Report AFWAL-TR-87-4060, Materials Laboratory, Air Force Wright Aeronautical Laboratories, Wright-Patterson AFB, July 1987.
- [19] Gilbert, C. J., McNaney, J. M., Dauskardt, R. H. and Ritchie, R. O., "Back-Face Strain Compliance and Electrical-Potential Crack Length Calibrations for the Disk-Shaped Compact-Tension DC(T) Specimen," *ASTM Journal Test. Eval.*, Vol. 22 No. 2, 1994, pp. 117-120.
- [20] Aronson, G. H. and Ritchie, R. O., "Optimization of the Electrical Potential Technique for Crack Growth Monitoring in Compact Test Pieces Using Finite Element Analysis," *ASTM Journal of Testing and Evaluation*, Vol. 7, No. 4, 1979, pp. 208-215.
- [21] Gilbert, C. J. and Ritchie, R. O., "Mechanisms of Cyclic Fatigue-Crack Propagation in a Fine-Grained Alumina Ceramic: Role of Crack Closure," *Fat. Fract. Eng. Mat. Struct.*, Vol. 20, No. 10, 1997, pp. 1453-1466.
- [22] Gilbert, C. J., Cao, J. J., MoberlyChan, W. J., De Jonghe, L. C. and Ritchie, R. O., "Cyclic Fatigue and Resistance-Curve Behavior of an In Situ Toughened Silicon Carbide with Al-B-C additions," *Acta Metall. Mater.*, Vol. 44, No. 8, 1996, pp. 3199-3214.
- [23] M. E. Sixta, X. F. Zhang, and L. C. De Jonghe, "Creep of SiC Sintered with Al, B, and C," submitted to *Journal Am. Ceram. Soc.*, 2000.
- [24] Chen, D., Gilbert, C. J., Zhang, X. F. and Ritchie, R. O., "High-Temperature Cyclic Fatigue-Crack Growth Behavior in an In Situ Toughened Silicon Carbide Ceramic," *Acta Mater.*, Vol. 48, No. 3, 2000, pp. 659-674.